

TIME-RESOLVED X-RAY DIFFRACTION:
STATISTICAL THEORY AND ITS APPLICATION
TO THE PHOTO-PHYSICS OF MOLECULAR
IODINE

S. Bratos⁽¹⁾, F. Mirloup⁽¹⁾, R. Vuilleumier⁽¹⁾ and M. Wulff⁽²⁾

⁽¹⁾ *Laboratoire de Physique Théorique des Liquides,*

Université Pierre et Marie Curie,

Case courrier 121, 4, Place Jussieu, 75252 Paris Cedex 05, France

⁽²⁾ *European Synchrotron Radiation Facility,*

BP 220, 6, rue Jules Horowitz,

Grenoble Cedex 38043, France

July 2, 2002

Abstract

A theory is proposed to study time-resolved X-ray diffraction on the pico- and subpicosecond time scales. Electromagnetic fields are treated in the frame of Maxwellian electrodynamics, whereas the molecular system is treated by using quantum mechanics. An expression is given for the time-resolved X-ray signal; it involves a three-time correlation function of the Fourier transformed electronic density and of the electric dipole moment of the system. This theory is applied to the study of the recombination of photo-dissociated iodine molecules in solution. Both geminate and non-geminate recombination are considered. The feasibility of the real time visualization of atomic motions is discussed.

1 Introduction

Real time observation of temporally varying molecular structures during an elementary chemical process represents an immense challenge for modern science. Several experimental techniques have been employed to accomplish this task. (i) Ultrafast spectroscopy, operating on the pico- and femtosecond time scales, permits the detection of various short lived species and the determination of their lifetimes^{1,2}. Unfortunately, visible light interacts predominantly with outer shell rather than with deeper lying core electrons that most directly indicate molecular geometry. It is thus difficult to convert spectral data into data on molecular geometry. (ii) Another technique is electron diffraction giving access to time domains extending from nano- to picoseconds^{3,4}. However, the electrons having a short penetration depth, this technique is more useful for studying gases and surfaces than for analyzing condensed matter. (iii) Finally, since their discovery, X-rays have always been the dominant tool for the determination of molecular structures⁵. If this technique is to be applied to the study of temporally varying molecular structures, pulsed X-ray sources are required; a number of technically very demanding constraints are imposed on pulse duration, brilliance and photon flux. Three main types of instruments are presently available. Laser-produced plasma sources generate very short picosecond pulses or below. Another X-ray source is synchrotron, which may produce high flux beams with pulses between 50 and 200 picoseconds with a well defined structure and polarization. Finally, X-ray diodes with a laser triggered photocathode may offer pulses between 10 and 100 picoseconds. Unfortunately, none of these sources meets all the requirements needed for a real time probing of molecular motions. The situation in this field at the present time recalls that of laser spectroscopy thirty years ago. However, instrumental developments are extremely fast, and the situation may evolve quickly.

The present paper deals with ultrafast time-resolved X-ray diffraction. It is important to realize that if the times involved in the experiment are of the order of, or shorter than molecular collision times, a new theory of time-resolved X-ray diffraction is called for. The usual procedure of treating the slowly varying X-ray diffraction consists in combining well known laws of chemical kinetics and of X-ray physics; this procedure fails at short times where rate constants lose their meaning. An entirely new theory is

then required, reminiscent of those familiar in ultrafast laser spectroscopy. Based on the correlation function approach, it employs systematically nonlinear response functions and susceptibilities; the latter are generally non-local in space and time. This approach, necessary when working in the pico- and femtosecond time domain, may occasionally be needed even at much longer times.

A number of ultrafast X-ray diffraction experiments have been realized the past few years; they may be sketchily described as follows. (i) Thermal effects in crystalline lattice, consecutive to the impact of an intense laser shot, were measured on the pico- and subpicosecond time scales. Non-thermal melting, lattice expansion, and heat or strain propagation were examined for crystals such as Au⁶, Ge⁷, GaAs⁸ and InSb⁹⁻¹¹. More complex structures like Langmuir-Blodgett films were also studied; a structural disorder and an expansion were observed in these films¹². (ii) Structural relaxation of the photoexcited 4-dimethylaminobenzonitrile (DMABN) was monitored with 100 picosecond time resolution. The excited state geometry was found similar to that present at low temperatures¹³. (iii) Particularly interesting are nanosecond X-ray diffraction studies of a number of biologically important crystals. One of them contains complexes formed by the myoglobin and carbon monoxide molecules. Changes of the crystal structure due to motions of this latter entity was observed^{14,15}. The yellow protein was also studied in its state [pR]; the presence of a photo-induced energy transfer was reported^{16,17}. (iv) All these papers refer to the solid phase; diffuse scattering of liquids was only very recently addressed. The geminate recombination of the photo-excited I₂ in CH₂Cl₂ was investigated at 100 picosecond time scales¹⁸. As this reaction is considered as a sort of prototype of a “simple” chemical reaction, it was extensively studied by ultrafast laser spectroscopy over many years and it is now reexamined by X-ray techniques. The conclusion is that in spite of a great progress, the field of ultrafast X-ray diffraction still is in an early state of development.

First theoretical attempts in the field of time-resolved X-ray diffraction were entirely empirical. More precise theoretical work appeared only in late 90’s, and is due to K.Wilson and his collaborators¹⁹⁻²¹; see also C.H. Chao et al.²² Their theory is based on the following assumptions. (i) The scattering process is described in terms of the first Born approximation and ignores absorption processes. (ii) The material system is quantum-mechanical and is treated by adopting the wave function approach. The Born-

Oppenheimer approximation and the independent atom model are used in this step. (iii) The laser emitted X-ray pulse is considered as an incoherent sum of ultrashort sub-pulses, the duration of which is determined by the properties of the X-ray source. (iv). The instantaneous diffraction signal, response of the system to each of those ultrashort X-ray sub-pulses, is calculated and is averaged over nuclear degrees of freedom. (v) The final signal intensity is determined by convoluting the instantaneous diffraction signal with the time envelope of the incident X-ray radiation. A number of predictions were made, based on numerical calculations^{19,23}.

This theory was the first to propose a tractable computational scheme. It also emphasized that the diffraction signal is not necessarily mere superposition of independent signals as interference effects may be present for short pulses in the case of the potential energy crossing. Moreover, an interesting suggestion was made to realize a nearly complete population inversion with positively chirped laser pulses; this procedure should permit to isolate the excited state dynamics from that characteristic of the ground state²⁴. The major disadvantage of the Wilson theory, in addition to that of introducing a number of assumptions, is that it is not a statistical theory. Modern work on condensed matter invariably employs the correlation function approach, both in linear and nonlinear spectroscopy². It is certainly well adapted to problems encountered in this field.

The purpose of the present paper is to develop a statistical theory of ultrafast X-ray diffraction in the condensed phases. It is based on the time scale separation between optical and X-ray frequencies; the X-ray and the optically triggered molecular processes are treated separately, one after the other. The first of these two steps is accomplished by adopting a Maxwellian description of X-ray scattering and the second is realized by using standard methods of statistical mechanics of nonlinear optical processes². The diffraction signal is expressed in terms of a three-time correlation function, which contains the Fourier transformed electron density and the dipole moment of the system. The theory is then applied to the study of the recombination of photo-dissociated I₂ in CH₂Cl₂, both geminate and non-geminate. The experimental information about this process is mainly due to the laser studies, although some preliminary time-resolved X-ray results are also available. The agreement with experimental data, as far as they are available, is very good; however, to a large extent, our results represent a theoretical prediction.

It should also be noted that our theory provides a convenient frame which facilitates the interpretation of time-resolved X-ray experiments and their comparison with laser data.

2 Basic Theory

2.1 Generalities

The system considered in this study is a solid or liquid material, containing N molecules in volume V . It is submitted to an intense optical pump pulse of frequency Ω which brings the system into a conveniently chosen initial state, for example a state in which a chemical reaction is initiated. At a later time, it undergoes the action of an X-ray probe pulse of intensity I_X which permits to measure its diffraction pattern and changes of molecular structure. The time delay between the optical pump pulse and the X-ray probe pulse is noted τ . These two pulses have in general a different polarization. The measured quantity is the signal ΔS , defined as time integrated X-ray energy flux S scattered in a solid angle in presence of the pump minus time integrated X-ray energy flux S_0 in a solid angle in the absence of the pump. The signal ΔS is thus a differential quantity.

The present experiment has two characteristic features which merit attention. The first is that the optical pump and the X-ray probe pulses have vastly different energies and wave lengths. The typical energy of photons in the optical pulse is of the order of a few eV, whereas that of photons in the X-ray pulse is in the keV range. A similar statement holds for the wave lengths, which are of the order of 10^3 Å for the optical pulse and of 1 Å for the X-ray pulse. This duality strongly influences the experimental work, requiring high energy techniques in the X-ray part of work and laser techniques in its optical part. On the contrary, the presence of this scale separation simplifies, rather than complicates, theoretical work. It makes the separate study of X-ray probing and of optical excitation possible, which reduces the complexity of the problem considerably.

The second major point is that the wave length λ of the optical radiation is much longer than molecular dimensions, but still much smaller than experimental cell dimensions. However, molecular motions are probed only over distances of the order of $l \ll \lambda$ (Fig. 1). A system experiencing a spatially varying electric field is then dynamically

equivalent to an ensemble of sub-systems submitted to a spatially constant electric field, different when going from one sub-system to another. The vector \mathbf{r} no longer denotes a space point, but selects a given sub-system. It is thus legitimate to work initially with a spatially constant electric field and to average the results over all sub-systems at the end of calculation. This point of view, although not always stated explicitly, is regularly employed in laser spectroscopy; it is also reminiscent of the theory of X-ray diffraction of powders.

These two features suggest the following route to build a theory of time-resolved X-ray diffraction. Its first step consists in developing a Maxwell-type theory of X-ray scattering by optically excited systems, and the second step in presenting a statistical description of pump-induced changes in the electron density. The final step consists in combining these results to obtain an expression for the differential signal ΔS . Absorption processes will be ignored all along in this paper. These three problems are studied separately in the subsequent parts of this Section.

2.2 Maxwellian Description of X-Ray Diffraction in Presence of Optical Excitation

The theory of X-ray scattering by a stationary system of atoms and molecules is developed in many textbooks²⁵. Its key quantity is the Fourier-transformed electron number density $\tilde{n}(\mathbf{q})$, which is independent of time. Using this theory permits to extract from the experimental diffraction pattern electronic densities as well as the geometrical structure of the crystal. In disordered systems like powders or liquids, the data are less complete but still remain very rich. A large body of information was accumulated in this way. However, if the system is submitted to an optical excitation, it no longer remains in thermal equilibrium, and the charge densities no longer are stationary. The Maxwell theory of X-ray scattering must thus be modified to include this specific feature.

As conventional in electromagnetism, the body under consideration is represented by a system of charges and currents. The corresponding densities $\rho(\mathbf{r}, t)$ and $\mathbf{J}(\mathbf{r}, t)$ are supposed to be known functions of \mathbf{r} and t . The incident X-ray electric and magnetic fields $\mathbf{E}(\mathbf{r}, t)$ and $\mathbf{H}(\mathbf{r}, t)$ are pulses having planar wave fronts; one has $\mathbf{E}(\mathbf{r}, t) = \mathbf{E}(\mathbf{r}, t) \exp(-i\omega t)$ and $\mathbf{H}(\mathbf{r}, t) = \mathbf{H}(\mathbf{r}, t) \exp(-i\omega t)$ where ω is the carrier frequency in the

keV range. As the purpose of the experiment is to monitor optically excited molecular motions in the system, the pulse duration should correspond to these. The amplitudes $\mathbf{E}(\mathbf{r}, t)$ and $\mathbf{H}(\mathbf{r}, t)$ are thus chosen to vary on optical time scales, long compared to $1/\omega$; it is then justified to neglect $\partial\mathbf{E}/\partial t$ and $\partial\mathbf{H}/\partial t$ as compared with $i\omega\mathbf{E}$ and $i\omega\mathbf{H}$. Moreover, the system being globally neutral, the total charge density ρ may be taken equal to zero. The current density $\mathbf{J}(\mathbf{r}, t)$ is given by the formula $\mathbf{J}(\mathbf{r}, t) = (ie^2/m\omega)n(\mathbf{r}, t)\mathbf{E}(\mathbf{r}, t)$, where e and m denote the electronic charge and mass, respectively, and $n(\mathbf{r}, t)$ their number density at point \mathbf{r} and time t ²⁵; this relation is valid if the X-ray frequencies are large as compared to the absorption edge frequencies in atoms⁵. The time dependence of $n(\mathbf{r}, t)$ is due to the optical excitation; since optical frequencies are small compared to X-ray frequencies, it must also be considered as a slow variable. Under these conditions, the Maxwell equations of the irradiated body are completely defined:

$$\text{div}\mathbf{E} = \mathbf{0}, \text{div}\mathbf{H} = \mathbf{0}, \text{rot}\mathbf{E} = -\frac{1}{c}\frac{\partial\mathbf{H}}{\partial t}, \text{rot}\mathbf{H} = \frac{4\pi}{c}\mathbf{J} + \frac{1}{c}\frac{\partial\mathbf{E}}{\partial t}. \quad (1)$$

Once these equations have been established and appropriate boundary conditions imposed, the problem reduces to that of searching for solutions which describe the scattered electromagnetic radiation in the far field limit. It is then convenient to introduce the electric displacement vector $\mathbf{D}(\mathbf{r}, t) = \epsilon(\mathbf{r}, t)\mathbf{E}(\mathbf{r}, t)$ where $\epsilon = 1 - (4\pi e^2/m\omega^2)n(\mathbf{r}, t)$ and to recast the Maxwell equations in order to obtain a wave equation for it. The procedure remains similar to that employed in the standard theory, except that the amplitudes $\mathbf{E}(\mathbf{r}, t)$, $\mathbf{H}(\mathbf{r}, t)$ and $n(\mathbf{r}, t)$ are now functions of time and not simply constant. There results:

$$\Delta\mathbf{D}(\mathbf{r}, t) - \frac{1}{c^2}\frac{\partial^2\mathbf{D}(\mathbf{r}, t)}{\partial t^2} = \text{rot rot} \left(\frac{4\pi e^2 n(\mathbf{r}, t)}{m\omega^2} \mathbf{E}(\mathbf{r}, t) \right). \quad (2)$$

On the right-hand side of this equation containing the small quantity $4e^2n(\mathbf{r}, t)/m\omega^2$, $\mathbf{E}(\mathbf{r}, t)$ must be taken as a given field of the incident wave. A solution which corresponds to an outgoing scattered wave may be obtained by the theory of retarded potentials²⁶. In fact, putting $\mathbf{E}(\mathbf{r}, t) = \mathbf{E}(\mathbf{r}, t) \exp(i(\mathbf{k}_I\mathbf{r} - \omega t))$ where \mathbf{k}_I is the wave vector of the incident radiation, introducing the effect of time retard not only in the phase factor $i(\mathbf{k}_I\mathbf{r} - \omega t)$ but also into the field amplitude $\mathbf{E}(\mathbf{r}, t)$, and employing well known formulas of the vector analysis, one finds

$$\mathbf{D} \left(\mathbf{R}_0, t + \frac{R_0}{c} \right) = \frac{e^2}{m\omega^2} \frac{e^{-i\omega t}}{R_0} \mathbf{k}_D \times \left[\mathbf{k}_D \times \mathbf{E}(t) \int n(\mathbf{r}, t) e^{-i\mathbf{q}\cdot\mathbf{r}} d\mathbf{r} \right]. \quad (3)$$

In this equation \mathbf{k}_D is the wave vector of the scattered radiation, $\mathbf{q} = \mathbf{k}_D - \mathbf{k}_I$ is the scattering wave vector, whereas \mathbf{R}_0 points from an arbitrarily chosen point inside the scattering body to the point of observation. It should be noted that the latter is located in the vacuum and thus $\mathbf{D} = \mathbf{E}$. In the case under consideration the incident radiation is pulsed, as is the scattered radiation; the corresponding intensities are angle and time-dependent. Then,

$$\begin{aligned}
S &= \int_{-\infty}^{+\infty} \frac{dI_S}{d\Omega} dt = \frac{cR_0^2}{4\pi} \int_{-\infty}^{+\infty} \mathbf{E}^*(t)\mathbf{E}(t) dt \\
&= \frac{cR_0^2}{4\pi} \int_{-\infty}^{+\infty} \mathbf{E}^*\left(t + \frac{R_0}{c}\right)\mathbf{E}\left(t + \frac{R_0}{c}\right) dt \\
&= \frac{c}{4\pi} \left(\frac{c^2}{m\omega^2}\right)^2 k_D^4 \sin^2 \theta \int_{-\infty}^{+\infty} \mathbf{E}^*(t)\mathbf{E}(t) \left| \int n(\mathbf{r}, t) e^{-i\mathbf{q}\cdot\mathbf{r}} d\mathbf{r} \right|^2 dt \\
&= \left(\frac{e^2}{mc^2}\right)^2 \sin^2 \theta \int_{-\infty}^{+\infty} I_X(t) f(t)f^*(t) dt,
\end{aligned} \tag{4}$$

where θ is the angle between \mathbf{E}_I and \mathbf{k}_D and $f(t) = \int d\mathbf{r} n(\mathbf{r}, t) \exp(-i\mathbf{q}\cdot\mathbf{r}) = \tilde{n}(\mathbf{q}, t)$ is the X-ray form factor. In an optically excited system brought out of thermal equilibrium, this latter quantity is expected from physical grounds to vary with time. However, the above result was obtained here formally by solving the Maxwell equations in the slowly varying amplitude limit; in earlier work this step was taken as granted a-priori and was not submitted to a formal check¹⁹⁻²¹. It should be stressed, however, that the simplicity of the result rests on the definition of the signal as a time-integrated quantity; it is lost otherwise, as seen by considering Eq. (3) and Eq. (4).

In practice, the incident X-ray radiation may be produced in different ways. If it is generated by a non-polarized source, the polarization factor $P = \sin^2 \theta$ has to be replaced by the factor $P = (1/2)(1 + \cos^2 \psi)$, where ψ denotes the angle between the wave vectors \mathbf{k}_I and \mathbf{k}_D . If a synchrotron source is employed, two situations are frequently encountered. The observation point may be located in the vertical scattering plane and the polarization factor P is then equal to 1; it may also be contained in the horizontal scattering plane where $P = \cos^2 \psi$. For more details, see Ref. [5].

2.3 Statistical Determination of the Time Dependent Form Factor

The Maxwell description of X-ray diffraction by an optically excited system, presented in the preceding Section, is incomplete. In fact, the temporally varying form factor $f(t)$ was considered as a known function, which is not true. It can be determined, however, by using methods of statistical mechanics of nonlinear optical processes². The quantity $f(t)f^*(t)$ should be averaged over all degrees of freedom of the perturbed system; this operation is denoted by the symbol $\langle \rangle$. Moreover, it is convenient to express the time delay τ between the optical pump and the X-ray probe pulse explicitly. The scattered X-ray intensity S can then be written:

$$S = \left(\frac{e^2}{mc^2} \right)^2 P \int_{-\infty}^{+\infty} I_X(t) \langle f(t+\tau)f^*(t+\tau) \rangle dt. \quad (5)$$

It is noteworthy that the only quantity in Eq. (5) referring to the X-ray scattering is I_X : the problems of X-ray scattering and of optical excitation have been disentangled from each other. The electric field to be considered from now on is the optical electric field $\mathbf{E}_O(\mathbf{r}, t)$; the subscript O is no longer necessary and will be suppressed in what follows; this simplification of the notation should introduce no confusion. The effect of the optical excitation on electronic densities has been studied by many authors, mostly in the context of laser spectroscopy². The methods used therein are easily transferable to the calculation of $\langle f(t+\tau)f^*(t+\tau) \rangle$, and will be employed in what follows.

Let then \mathcal{H}_0 denote the quantum mechanical Hamiltonien of the system in absence of any perturbation. At large negative times $t \rightarrow -\infty$, the sample is submitted to an intense electric field $\mathbf{E}(\mathbf{r}, t)$ having, as indicated earlier, a constant amplitude inside the system. If the dipolar approximation is employed, the perturbation Hamiltonien takes the form $\mathcal{H}_1 = -M_i E_i$, where M_i and E_i are the components of the vectors \mathbf{M} and \mathbf{E} along the axis i ; the Einstein convention is employed all along, involving a summation over the doubled indices. The complete Hamiltonien of the system is then $\mathcal{H} = \mathcal{H}_0 + \mathcal{H}_1$. To execute the operation $\langle \rangle$ in Eq.(5), the density matrix $\rho(t)$ of the perturbed system is required. It can be obtained by solving von Neumann's equation $\partial\rho/\partial t = -(i/\hbar) [\mathcal{H}, \rho]$ by the help of the perturbation theory. One can then write $\rho = \rho_0 + \rho_1 + \rho_2 + \dots$ where $\rho_0, \rho_1, \rho_2, \dots$ are successive corrections of ρ . Choosing the equilibrium density matrix

ρ_0 in the canonical form, one finds

$$\begin{aligned}\rho_1(t) &= i \int_0^{+\infty} E_i(\mathbf{r}, t - \tau_1) e^{-i\mathcal{L}_0\tau_1} \mathcal{L}_{1i} \rho_0 d\tau_1 \\ \rho_2(t) &= i^2 \int_0^{+\infty} \int_0^{+\infty} E_i(\mathbf{r}, t - \tau_1) E_j(\mathbf{r}, t - \tau_1 - \tau_2) \\ &\quad \times e^{-i\mathcal{L}_0\tau_1} \mathcal{L}_{1i} e^{-i\mathcal{L}_0\tau_2} \mathcal{L}_{1j} \rho_0 d\tau_1 d\tau_2,\end{aligned}\tag{6}$$

where $\mathcal{L}_0 = (1/\hbar) [\mathcal{H}_0, \]$ is the non-perturbed Liouville operator of the system, $\mathcal{L}_{1i} = (1/\hbar) [M_i, \]$ and $[\ , \]$ a commutator. The above determination of the perturbed density matrix constitutes the first step of calculation.

Once this important step was accomplished, the quantum operator for the scattering factor $f(t)$ must be defined. The central dynamical variable of the present theory is the electron density $n(\mathbf{r}, t)$. In microscopic language, the quantity $n(\mathbf{r}, 0) = n(\mathbf{r})$ can be written $n(\mathbf{r}) = \sum \delta(\mathbf{r}_m - \mathbf{r})$ where \mathbf{r}_m denotes the position of the electron m , the summation running over the N_e electrons of the scattering system; $n(\mathbf{r}, t)$ is then equal to $\exp(i\mathcal{H}_0 t/\hbar) n(\mathbf{r}) \exp(-i\mathcal{H}_0 t/\hbar)$. The form factor is its Fourier transform $f = \int d\mathbf{r} \exp(-i\mathbf{q}\mathbf{r}) \sum \delta(\mathbf{r}_m - \mathbf{r}) = \sum \exp(i\mathbf{q}\mathbf{r}_m)$; $f(t)$ can then be written $\exp(i\mathcal{H}_0 t/\hbar) f(\mathbf{q}) \exp(-i\mathcal{H}_0 t/\hbar)$. The time is introduced into the calculation through the time dependent density matrix $\rho(t)$ given above. Then,

$$\begin{aligned}\langle f(t) f^*(t) \rangle &= Tr \left(\sum e^{-i\mathbf{q}\cdot\mathbf{r}_{mn}} \rho(t) \right) = Tr \left(\sum e^{-i\mathbf{q}\cdot\mathbf{r}_{mn}} \rho_0 \right) \\ &\quad + Tr \left(\sum e^{-i\mathbf{q}\cdot\mathbf{r}_{mn}} \rho_1 \right) + Tr \left(\sum e^{-i\mathbf{q}\cdot\mathbf{r}_{mn}} \rho_2 \right) + \dots\end{aligned}\tag{7}$$

where \mathbf{r}_{mn} denotes a vector pointing from the electron m to the electron n . The problem then reduces to that of substituting the expressions for ρ_0 , ρ_1 and ρ_2 into Eq. (7) and rearranging the resulting formulas. Considering the properties of higher order correlation functions vis-a-vis time shift and time inversion facilitates the reduction and the transformation of various mathematical expressions involved.

In the above calculations, the optical pump electric field $\mathbf{E}(\mathbf{r}, t)$ was considered to be spatially constant. However, according to the discussion given in Section 2.1 and illustrated in Fig. (1), this assumption in reality holds true only for individual sub-systems into which the system was decomposed, and does not apply to the system as a whole. To reach the end result, it is still necessary to average the above expressions

over all sub-systems. In addition, the incident optical field is never entirely coherent and always has at least some stochastic characteristics. It is thus necessary to average, not only over different subsystems, but also over different realizations of the incident optical field. Clumped together, these two operations will be denoted by the symbol $\langle \rangle_O$. Another operation which is required is the averaging over the states of the non-perturbed system and is denoted by the symbol $\langle \rangle_S$. These two operations are of course independent of each other. Then, recalling that $\mathbf{E}(\mathbf{r}, t)$ is a progressive wave and that its average $\langle \rangle_O$ over the whole system vanishes, one obtains:

$$\begin{aligned} \langle f(t)f^*(t) \rangle = & \left\langle \sum e^{-i\mathbf{q}\cdot\mathbf{r}_{mn}(0)} \right\rangle_S - \frac{1}{\hbar^2} \int_0^{+\infty} \int_0^{+\infty} \left\langle E_i(\mathbf{r}, t - \tau_1) E_j(\mathbf{r}, t - \tau_1 - \tau_2) \right\rangle_O \\ & \times \left\langle \left[\left[\sum e^{-i\mathbf{q}\cdot\mathbf{r}_{mn}(\tau_1+\tau_2)}, M_i(\tau_2) \right], M_j(0) \right] \right\rangle_S d\tau_1 d\tau_2 \quad (8) \end{aligned}$$

2.4 Statistical Expression for the Diffracted Signal

The final expression for the signal recorded in a time-resolved X-ray experiment can now be written by combining partial results of Sections 2.2 and 2.3. In fact, inserting Eq. (8) into Eq. (5) and recalling that $\Delta S = S - S_0$, where S is the time integrated diffraction intensity in presence of optical excitation and S_0 is the time integrated diffraction intensity in its absence, there results:

$$\begin{aligned} \Delta S(\mathbf{q}, \tau) = & \int_{-\infty}^{+\infty} I_X(t - \tau) \Delta S_{inst}(\mathbf{q}, t) dt \\ \Delta S_{inst}(\mathbf{q}, t) = & - \left(\frac{e^2}{mc^2\hbar} \right)^2 P \int_0^{+\infty} \int_0^{+\infty} \left\langle E_i(\mathbf{r}, t - \tau_1) E_j(\mathbf{r}, t - \tau_1 - \tau_2) \right\rangle_O \quad (9) \\ & \times \left\langle \left[\left[\sum e^{-i\mathbf{q}\cdot\mathbf{r}_{mn}(\tau_1+\tau_2)}, M_i(\tau_2) \right], M_j(0) \right] \right\rangle_S d\tau_1 d\tau_2. \end{aligned}$$

This is the main result of this work: $\Delta S(\mathbf{q}, t)$ as given by Eq. (9) represents the statistical expression for the diffracted signal which was desired. Its general form can be easily understood. The basic dynamical variable involved in X-ray scattering is the Fourier transformed electron density; the presence of the factor $f(\tau_1 + \tau_2)f^*(\tau_1 + \tau_2) = \sum \exp[-i\mathbf{q}\cdot\mathbf{r}_{mn}(\tau_1 + \tau_2)]$ is thus inevitable. The remaining quantities in Eq.(9) describe the effect of the optical excitation. In fact, according to the Fermi golden rule, the rate of this excitation is $\sim 1/\hbar^2(\mathbf{E}\mathbf{M}_if)^2$ which explains the presence of the factors $1/\hbar^2$, $E_i(t - \tau_1)$, $E_j(t - \tau_1 - \tau_2)$, $M_j(0)$ and $M_i(\tau_2)$. The connection of different time

points can of course not be explained that simply. Finally, the signal ΔS appears as a convolution between the X-ray pulse shape I_X and the quantity ΔS_{inst} , the diffraction signal generated by an infinitely short X-ray probe pulse. It should be stressed that this is a genuine result of the theory, and is not a consequence of an ad hoc assumption.

Another major feature of the above result is the presence therein of three-time correlation functions, associated with the variables $\tilde{n}(\mathbf{q})$, \mathbf{M} and \mathbf{E} , respectively. These objects are characteristic of statistical mechanics of non-equilibrium systems. If the perturbation generating the non-equilibrium is weak, two-time correlation functions suffice; this is the case for all types of linear spectroscopy. If the perturbation is stronger, higher-order time correlation functions appear: three-time correlation functions are present in Eq. (9), four-time correlation functions are required in pump-probe experiments in laser spectroscopy, etc. Nevertheless, the structure of the resulting expressions for the signal is similar everywhere. The expression for ΔS provided by this theory is thus conforming to the existing body of information and its form is by no means a surprise.

It should finally be emphasized that the signal ΔS of Eq. (9) depends, not only on the properties of the material submitted to investigation, but also on those of the incident optical wave. The latter determines the structure of the electric field correlation function, and thus the characteristics of the resulting signal. The effects of coherence or incoherence of the pump radiation can be treated on this level of the theory. The signal is non-vanishing even at small negative times; this is a consequence of the overlap between the pump and probe pulses. It should also be noted that optical pumping modifies not only the coherent, but also the incoherent Compton component of the scattered X-ray radiation; this effect does not play any role in the subsequent analysis, but may be important in some cases. All these various effects are describable by Eq. (9), which shows its generality.

3 Recombinaison of molecular iodine in solution

3.1 Basic Information

The theory which was described above will now be applied to the study of the geminate and non-geminate recombination of photo-dissociated iodine molecules diluted in

CH₂Cl₂. This reaction has been considered over many years as a “simple” chemical reaction, and has therefore been carefully examined by laser spectroscopic techniques. Here it will be reexamined using time-resolved X-ray diffraction techniques; for a review of recent technical developments, see Ref. [27]. One started by exciting the solution with a laser generated optical pulse, bringing the iodine molecule into the electronic states B and $^1\pi_u$ (Fig. 2). The molecule then dissociates very rapidly, in times of the order of a picosecond. The hot atoms recombine, in part geminately and in part non-geminately. The former process requires 500 ps whereas the latter takes place on the microsecond time-scale; these numbers are known from laser spectroscopy^{28–31}. The recombination processes were monitored using a time delayed X-ray probe pulse from the synchrotron. The duration of the optical pump pulse τ_O was 150 fs and that of the X-ray pulse τ_X was 80 ps. The pump and probe sequence was repeated at 896.6 Hz and the diffuse scattering was recorded on a CCD based area detector placed downstream the sample¹⁸. Although comparatively long due to technical constraints, τ_X still was short enough to follow the recombination processes between 100 ps and a microsecond. The purpose of this work is to interpret the existing X-ray data; theoretical predictions will also be given.

3.2 Theoretical Analysis

It is convenient to start by giving a short description of times characteristic of a time-resolved X-ray diffraction experiment; four of them merit particular attention. The first two are the optical pump pulse duration τ_O and the X-ray probe pulse duration τ_X . According to basic principles of physics, it is impossible to follow molecular motions at time scales much shorter than the pulse duration, i.e. much shorter than τ_O and τ_X . The dynamics associated with them are not detectable by the experiment. The third characteristic time is the relaxation time τ_R of molecular rotations. At times shorter than τ_R the pump electric field induces a partial alignment of molecular orientations in the scattering body; this alignment is entirely lost if $\tau \gg \tau_R$. One concludes that the diffraction pattern depends on the mutual orientation of the vectors \mathbf{q} and \mathbf{E} if $\tau \ll \tau_R$; on the contrary, polarization effects are absent if $\tau \gg \tau_R$. The last characteristic time $\tau_I = 1/\Delta\omega$ is related to the vibrational interference of two closely lying electronic states, separated by an energy gap $\Delta E = \hbar\omega$. This interference generates beating phenomena,

similar to those observed in laser spectroscopy; the crests in time plots are separated by an interval equal to τ_I . However, if either $\tau_O \gg \tau_I$ or $\tau_X \gg \tau_I$, this oscillating component averages out to zero and the diffraction pattern reduces to a superposition of individual patterns. More generally, several electronic states may interact and a group of τ_I 's may exist.

Which are the times that intervene in the present experiment? How do they compare with the time scales mentioned above? As τ_X is 80 ps, only the slow recombination dynamics are detectable and the fact that τ_O is much shorter does not alter this conclusion. On the other hand, τ_R is of the order of a few picoseconds. This time is very short as compared with τ_X , and the liquid can be considered as isotropic; no polarization effects are expected. Finally, in the range of inter-atomic distances submitted to investigation, the times τ_I are extremely short as compared with τ_X ; vibrational interference of different electronic states thus plays no role. It is useful to introduce a new molecule I_2^* resulting from dissociation of photo-excited I_2 ; setting its length to $R_0 = 4 \text{ \AA}$ is arbitrary to a certain extent, but small variations of it are irrelevant at time scales of the experiment. The recombination process under study can then be modeled as a chemical reaction in which I_2^* undergoes either the transformation $I_2^* \longleftrightarrow 2I$ or the transformation $I_2^* \longleftrightarrow I_2$ where I_2 is the ground state iodine molecule with $R_X = 2.67 \text{ \AA}$; see Fig. 2. The first of these two reactions leads – sooner or later – to non-geminate recombination, whereas the second represents geminate recombination. The energy deposited by the laser excitation leaves the I_2^* molecule hot, with all closely spaced electronic states populated. This picture has many advantages: starting the calculation immediately after photo-excitation would require a major effort to describe the passage of the system through energy crossing points, its pre-dissociation, etc. As these processes all evolve on the picosecond time scale, they are not accessible to this experiment; an effort to study them would thus not be justified.

Under these experimental conditions, the signal ΔS of Eq. (9) simplifies considerably. In fact, if reaction dynamics is followed on time scales beyond 100 ps, and the optical excitation processes evolve on a 1 ps time scale, the reaction driven electron density $\tilde{n}(\mathbf{q})$ and the dipole moment \mathbf{M} are statistically independent; they can thus be treated separately. Moreover, as beating phenomena can not be observed with the presently available experimental set-up, non-diagonal matrix elements of the variable $\tilde{n}(\mathbf{q})$ can

safely be omitted. Finally, the calculation can be simplified further by noticing that, with the exception of electronic degrees of freedom, the system behaves classically; the separation of highly excited vibrational energy levels of I_2 is much smaller than $k_B T$, which justifies this statement. Then, designating by f_I the form factor of atomic iodine, the same in the all electronic states considered, and by $n_j(t)$ the population of the electronic state j at time t ; and denoting by \sum the summation over the N_n nuclei located at \mathbf{r}_μ and \mathbf{r}_ν where $\mathbf{r}_{\mu\nu} = \mathbf{r}_\mu - \mathbf{r}_\nu$, and by $\langle \rangle_j$ the average over the nuclear degrees of freedom in the electronic state j , one finds:

$$\begin{aligned} \Delta S(\mathbf{q}, \tau) &= \int_{-\infty}^{+\infty} I_X(t - \tau) \Delta S_{inst}(\mathbf{q}, t) dt \\ \Delta S_{inst}(\mathbf{q}, t) &= \left(\frac{e^2}{mc^2} \right)^2 f_I^2 P \\ &\quad \times \sum_j \left[n_j(t) \sum_{\mu, \nu} \left(\langle e^{-i\mathbf{q} \cdot \mathbf{r}_{\mu\nu}(t)} \rangle_j - \langle e^{-i\mathbf{q} \cdot \mathbf{r}_{\mu\nu}(t)} \rangle_0 \right) \right] \\ n_j(t) &= 2Re \left[\frac{1}{\hbar^2} \int_0^{+\infty} \int_0^{+\infty} \langle E(\mathbf{r}, t - \tau_1) E(\mathbf{r}, t - \tau_1 - \tau_2) \rangle_O \right. \\ &\quad \left. \times \langle M_{oj}(\tau_2) M_{jo}(0) \rangle_S d\tau_1 d\tau_2 \right], \end{aligned} \tag{10}$$

where E is the pump electric field and M the component of \mathbf{M} along \mathbf{E} .

The physical meaning of Eq. (10) is as follows. After optical excitation, $n_j(t)$ molecules are promoted into the state j ; their contribution to the diffracted signal is equal to $n_j(t) \langle \exp(-i\mathbf{q} \cdot \mathbf{r}(t)) \rangle_j$. This promotion generates a population deficit, or a hole, in the ground electronic state equal to $-\sum_j n_j(t)$; its contribution to the signal is $-\left[\sum_j n_j(t) \right] \langle \exp(-i\mathbf{q} \cdot \mathbf{r}_{\mu\nu}(t)) \rangle_0$. The differential signal ΔS of Eq. (10) can then be viewed as a normal signal S by simply adding the hole to the existing particles; this picture greatly simplifies the discussion. It is also worth noting that Eq.(10) is similar to that proposed by Wilson et al. However, it is only valid if the restrictive conditions enumerated above are fulfilled; it has by no means the general character of Eq. (9).

3.3 Model

The following model can now be proposed to study the reactions $I_2^* \longleftrightarrow 2I$ and $I_2^* \longleftrightarrow I_2$; they are both supposed to start at time $\tau = 0$. (i) The electronic states which inter-

vene in the process are those where the iodine molecule dissociates into atoms in their $^2P_{3/2}$ state (Fig. 2). There are ten altogether: three of them, the ground state X and the states A/A' are attractive, whereas the seven others, including the $^1\pi_u$ state, are repulsive³². (ii) Several recombinaison pathways are available, see figure 3. The reaction $I_2^* \leftrightarrow 2I$ corresponds to the escape from the solvent cage and eventually leads to the non-geminate recombination. This process involving the seven non-bonded electronic states just mentioned, is called α . As far as the reaction $I_2^* \longleftrightarrow I_2$ is concerned, it may be realized in two different ways: either indirectly by trapping into the bound states A/A' and subsequent de-excitation to the ground state X, or directly by vibratonal de-excitation in the X state. These two processes are called β and γ , respectively. (iii) The total initial population of the seven nonbonded states is equal to n_α , the total initial population of the two bound states A/A' is equal to n_β and the initial population of the extended X state is equal to n_γ . These three numbers define the initial state of the hot I_2^* molecule. (iv) The decay of these populations is exponential for the processes α and β with time constants τ_n and τ_{isc} ; the first subscript refers to non-geminate recombination, and the second to inter-system crossing between the electronic states X and A/A' of different multiplicity. As far as the γ process or vibrational cooling of the X-state is concerned, it is in the heart of the present study. Its decay is thus described more precisely using a computer calculated radial distribution function $\rho_X(R, t)$ that obeys the initial condition $\rho_X(R, 0) = \delta(R - R_0)$ with $R_0 = 4 \text{ \AA}$. (iii) The quantities $\langle \exp(-i\mathbf{q}\mathbf{r}_{\mu\nu}) \rangle$ are calculated by averaging over an isotropic ensemble. This generates terms of the form $\sin(qR)/(qR)$, valid even if R is time-dependent and $R = R(t)$. These terms may be neglected in repulsive electronic states where interatomic separations are large. The final result is

$$\begin{aligned} \Delta S_{inst}(\mathbf{q}, t) = & 2 \left(\frac{e^2}{mc^2} \right)^2 f_I^2 P \\ & \times \left\{ -\xi_E(\tau) \frac{\sin(qR_X)}{qR_X} + \xi_{A/A'}(\tau) \frac{\sin(qR_{A/A'})}{qR_{A/A'}} \right. \\ & \left. + \xi_X \left[\int_0^{+\infty} 4\pi r^2 \rho_X(r, t) \frac{\sin(qr)}{qr} dr \right] \right\}, \end{aligned} \quad (11)$$

where $\xi_E(\tau) - n_\gamma = n_\alpha \exp(-\tau/\tau_n) + n_\beta \exp(-\tau/\tau_{isc})$ indicates the fraction of electronically excited I_2 molecules, $\xi_{A/A'}(\tau) = n_\beta \exp(-\tau/\tau_{isc})$ denotes the fraction of I_2 molecules captured in the two states A/A', whereas $\xi_X = n_\gamma$ is the fraction at the initial time $\tau = 0$

of I₂ molecules in the extended X state with $R = R_0 = 4 \text{ \AA}$. Moreover, R_X and $R_{A/A'}$ are the interatomic separations in the states X and A/A', equal to 2.67 and 3.01 \AA , respectively.

Finally, there still remains to describe how the radial density function $\rho_X(R, \tau)$ was determined from Molecular Dynamics simulations. Samples containing 512 or 216 rigid solvent molecules and one flexible I₂ molecule were considered at the experimental solvent density and at ambient temperature ($\rho = 1.33 \text{ g.cm}^{-3}$, $T = 300 \text{ K}$). They were first equilibrated for 500 ps; 10 configurations 10 ps apart were then extracted from a 100 ps long trajectory. In each of these configurations the iodine molecule was stretched from the equilibrium distance to $R_0 = 4 \text{ \AA}$ and the system was let to relax towards equilibrium in micro-canonical runs of 100 ps. $\rho_X(R, \tau)$ was then calculated as the distribution of R averaged over the 10 independent runs in a time window of 1 ps around τ . A three-site model composed of CH₂ and Cl units was employed for the dichloromethane molecules with a site-site 6-12 Lennard-Jones interaction potential³³. These molecules were kept rigid using the SHAKE/RATTLE method³⁴. The intramolecular Morse potential of I₂ was taken from ref. 35 and Lennard-Jones potentials between iodine atoms and solvent sites were constructed using the Lorentz-Berthelot formula with the parameters taken from ref. 36. In all simulations, a time-step of 1 fs was used. Further details will be published in a forthcoming paper³⁷. The simulations were repeated with $R_0 = 5 \text{ \AA}$. As this change did not affect the results to any significant extent, no further attempt was made to study physically more appropriate distributions of R_0 .

Although these simulations rely on an empirical potential, an important outcome of the calculation was that the iodine atoms stay a relatively long time at the turning points of the X-state potential. Consequently, the analysis can be simplified, while maintaining a high accuracy, by assuming that the iodine atoms are located at those turning points. Then, supposing for simplicity a mono-exponential energy decay of the form $U = D \exp(\tau/\tau_v)$, one finds easily:

$$U = D (1 - e^{-b(\Delta R)})^2 \Rightarrow \Delta R = -\frac{1}{b} \ln \left(1 \pm \sqrt{\frac{U}{D}} \right) \quad (12)$$

$$U(\tau) = D e^{-\frac{\tau}{\tau_v}}, \quad \Delta R(\tau) = -\frac{1}{b} \ln \left(1 \pm e^{-\frac{\tau}{2\tau_v}} \right),$$

where $\Delta R = R - R_X$, $D = 1.55 \text{ eV}$ the dissociation energy of molecular iodine and

$b = 1.91 \text{ \AA}^{-1}$ a constant³⁵; this formula can be easily extended to the case of a two-exponential energy decay. The X-ray diffraction pattern at time τ can thus be calculated by assimilating the recombining I atoms to two diatomic molecules with atoms separated by $R_X + \Delta R_+(\tau)$ or $R_X + \Delta R_-(\tau)$, and by combining Eq. (11) and Eq. (12). These calculations were realized up to $\tau = 100$ ps. The results are illustrated in Fig. 4 for $\tau = 1$ ps and $\tau = 25$ ps; the difference between simulations and model calculations becomes negligible for $\tau > 25$ ps. In view of their quality, this model has been used in all subsequent calculations.

3.4 Experimental Data and Theoretical Predictions

The theory has now attained a stage where it can produce explicit predictions and facilitate the analysis of the existing experimental data. The diffraction signals depend on two variables, the wave vector \mathbf{q} and the pump-probe time delay τ . Time-resolved X-ray diffraction is thus a two-dimensional technique, in the same sense as multidimensional NMR or multidimensional laser spectroscopy. It is then useful to distinguish between \mathbf{q} -resolved and τ -resolved diffraction patterns. Of course, a complete collection of \mathbf{q} -resolved diffraction patterns contains exactly the same information as the full collection of τ -resolved diffraction patterns. However, one never has at one's disposal all of them. Using a CCD detector, one collects \mathbf{q} -resolved patterns at a limited number of time points, whereas a point detector is more suitable for time scans at a limited number of \mathbf{q} -points. It is thus useful to examine each of them separately.

Let us study the τ -resolved diffraction patterns first; they are easier to analyze than their \mathbf{q} -resolved analogues. As indicated earlier, the calculations were realized for the solution $\text{I}_2/\text{CH}_2\text{Cl}_2$ where experimental X-ray data are partially available. Time constants were taken from the laser experiments^{28–31}: τ_n was chosen equal to $1 \mu\text{s}$, τ_{isc} to 0.51 ns and τ_v to 0.09 ns . The initial populations n_α , n_β and n_γ were estimated from the X-ray data: $n_\alpha = 0.05$, $n_\beta = 0.25$ and $n_\gamma = 0.25$ ¹⁸. Applying Eq. (11) then provided theoretical curves, which were compared with experimental curves when the latter became available. (i) Time-resolved diffraction pattern calculated with $q = 4\pi \sin \theta / \lambda = 2 \text{ \AA}^{-1}$ are illustrated in Fig. 5.a. Considered as a function of τ the signal $\Delta S(\mathbf{q}, \tau)$ first exhibits a steep rise corresponding to the build-up of the excited state populations; the zero time delay $\tau = 0$ is placed at its half-maximum. Its slope depends on the pump and probe

pulse duration τ_X and τ_O : shorter pulses produce steeper curves. After having reached its maximum, $\Delta S(\mathbf{q}, \tau)$ decreases monotonously. In its first 0.1 ns portion, the decay of the signal is governed by the process γ ; however, as τ_X is comparatively long, it manifests itself only to a minor extent. The next portion of the curve, from approximately 0.1 ns to 1 ns, is dominated by the process β . Finally, its last portion corresponds to time delays longer than 1 ns; the signal is influenced basically by the slow process α .

(ii) Absolute intensities of the signals as well as relative amplitudes of their components strongly depend on the choice of \mathbf{q} . For example, if $q = \pi/R_X = 1.58 \text{ \AA}^{-1}$, $\Delta S(\mathbf{q}, \tau)$ is very weak but the contribution of the process γ is relatively prominent (Fig. 5.b). (iii) Even the sign of the signal is \mathbf{q} -dependent (Fig. 5.c). The overshoot from negative to the positive values when passing from short to long time delays is possible as in laser spectroscopy. Experimental data are only available for the time domain $\tau < 0.6$ ns; they are illustrated on the last of the above three figures. The characteristic features seen in the experiment are similar to those predicted by theory.

The \mathbf{q} -resolved diffraction patterns are examined next. The time constants τ_n , τ_{isc} and τ_v as well as the initial populations n_α , n_β and n_γ are the same as above. The amplitude of the signal $\Delta S(\mathbf{q}, t)$ decreases with increasing time delay τ : the concentration of all excited molecular species including the hole decreases with time. Down to very small values of q , $\Delta S(\mathbf{q}, t)$ is non-zero, due to the decorrelation of free I atoms motions in process α . Other comments are as follows. (i) The \mathbf{q} -resolved diffraction pattern calculated for $\tau = 2$ ns is illustrated in Fig. 6.a. As this time is much longer than any other time except τ_n , only the hole is present due to the existence of free iodine atoms. The signal is then particularly simple and depends only on the initial distance $R_X = 2.67 \text{ \AA}$; it is representative of the α process. (ii) The diffraction pattern is next calculated for $\tau = 0.2$ ns (Fig. 6.b). In this case the A/A' molecules are present in the mixture in addition to the hole. The oscillations in the diffraction pattern thus exhibit two distances, $R_X = 2.67 \text{ \AA}$ and $R_{A/A'} = 3.01 \text{ \AA}$. This pattern is representative of the processes α and β . (iii) Finally, the diffraction pattern expected at $\tau = 0.0$ ns is calculated too (Fig. 6.c). The molecules A/A' and the extended X state molecules are then present in the system in addition to the hole. The diffraction pattern in this case is at its maximal complexity and brings out the distances $R_X = 2.67 \text{ \AA}$, $R_{A/A'} = 3.01 \text{ \AA}$ and $R(t)$. This latter quantity refers to the temporally varying iodine-iodine distance during

the process γ . Determining it for various time delays thus permits, in principle, real time visualization of atomic motions during this process. Practical possibilities of realizing the experiment are discussed below. Experimental data are only available for times of the order of 0.2 ns. Illustrated on Fig. 5.b, they show here again an overall agreement between experiment and theory. It is worth noting that this agreement is not affected by the presence of iodine-solvent cross terms. These terms are expected to be small since $f_{Cl} = f_I/3$ and $f_C = f_I/9$ for forward scattering and both fall off more rapidly than f_I with increasing θ . Indeed, they were shown from our Molecular Dynamics simulations to be completely negligible in $\Delta S(\mathbf{q}, t)$ for q larger than 0.5 \AA^{-1} .³⁷ They were thus not included into this model. Other secondary processes like laser heating of the sample have neither been considered.

Let us now come back to the major question whether, or not, it is possible with presently available techniques to “film” the atomic recombination in real time. The answer is certainly no as far as the processes α and β are concerned; the signals do not have a form appropriate for this sort of study. On the contrary, the visualization of these motions is perhaps possible for the process γ , i.e. recombination through vibrational relaxation in the X state. The \mathbf{q} -resolved signals were thus calculated for the I_2/CCl_4 solution in a time interval between 0 and 500 ps. All relaxation processes are slower in the solution I_2/CCl_4 than in $\text{I}_2/\text{CH}_2\text{Cl}_2$, and the chances of success seem more substantial here. Time constants were extracted from the laser spectroscopic experiments^{28–31}: τ_n was equal to 10 μs , τ_{isc} to 2.7 ns and τ_v to 0.175 ns. The initial populations n_α , n_β and n_γ are not known and the calculations were done with $n_\alpha = 0.05$, $n_\beta = 0.20$ and $n_\gamma = 0.20$; this estimate is only tentative. Some \mathbf{q} -resolved diffraction patterns calculated in this way are illustrated on Figs. 7.a,b. The effect of the finite X-ray pulse duration may be estimated by comparing these two figures. The peaks in the $1.5\text{--}5.0 \text{ \AA}^{-1}$ region, positive or negative, undergo shifts to higher \mathbf{q} values when τ increases from 0 to 500 ps. They are due to the shortening of I_2^* during the reaction $\text{I}_2^* \rightarrow \text{I}_2$. The calculated values of the \mathbf{q} shifts are of the order of 0.30 \AA^{-1} . The effect of convolution is to blur dynamical information to a certain extent. It results that “filming” iodine molecule during a vibrational relaxation is on the verge of feasibility with presently available techniques. The problem thus merits further consideration.

4 Discussion

The comparison with published data brings out the following points. The first concerns the theory by Wilson et al.^{19–23} The main feature common to their and our work is that electromagnetic fields are treated by Maxwellian electrodynamics, whereas the material system is described by quantum mechanics. There are also important differences, particularly in the way statistical aspects are handled. A wave function approach was adopted by Wilson, whereas the density matrix technique is employed here. As this latter technique is particularly powerful, a number of assumptions needed by Wilson are not required here. For example, the fact that the signal $\Delta S(\mathbf{q}, \tau)$ is a convolution of an X-ray pulse of finite width with a signal $\Delta S_{inst}(\mathbf{q}, \tau)$ corresponding to an infinitely short X-ray pulse, is an assumption in Wilson’s work and a theory generated result for us. Moreover, there is no need in the present work to assume that the X-ray pulse is a superposition of a great number of statistically independent components. The two theories lead in some cases to different predictions. The most important of them is that, according to Wilson’s theory, in absence of beating phenomena, the signal is a superposition of signals from different species in the system; the intensity of the component j is proportional to the fraction $n_j(t)$ of molecules in this state. In our theory this is true only at long times when the optical excitation processes are decoupled from the reactive processes. Beating phenomena are described similarly in both works.

The second point concerns a new paper on time-resolved X-ray spectroscopy, just published by Mukamel et al.³⁸ It appeared when our work was already written; nevertheless, the following comments seem appropriate. Its main theme is the study of extended X-ray absorption fine structure (EXAFS) and of related phenomena. Electromagnetic fields and molecular systems, and not only molecular systems, are treated in the frame of quantum mechanics. The time scale separation of X-ray and optical processes is considered too, although differently than here. The main difference between the two papers is in the way the electronic density changes are treated. In Mukamel et al. work they are calculated by statistical mechanics for both X-ray and optical excitations. In our work, the former are included in Maxwell’s treatment of X-ray scattering, whereas the latter are calculated by statistical mechanics. It can safely be stated that these two theories are largely complementary.

The present paper may be concluded by quoting Rentzepis et al.³⁹: The field of time-resolved X-ray diffraction and spectroscopy has made significant progress in the past decade. The advances in source technology have stimulated a wide variety of novel experiments using both synchrotrons and smaller laboratory size systems. They made possible the direct detection and assignment of ultrafast structures during the course of a photo-physical, chemical, or biological process. In favorable circumstances, time-resolved X-ray diffraction experiments may provide real time “snapshots” of temporally evolving molecular structures, which is a major challenge of the modern science. However, this field still is at an early stage of its development, from both experimental and theoretical point of view. Though, a rapid progress of this domain may be hoped for the present decade.

Acknowledgments

The authors acknowledge gratefully the support of the GDR 1017 of the CNRS during this work. They would also like to thank Ph. Anfinrud, F. Schotke, S. Techert and R. Neutze for stimulating discussions. The Laboratoire de Physique Théorique des Liquides is “Unité Mixte de Recherche” No. 7600 of the CNRS.

References

- [1] Y. R. Shank , The Principles of Nonlinear Optics, John Wiley & Sons (New York, 1984).
- [2] S. Mukamel, Nonlinear Optical Spectroscopy (Oxford University Press, New York, 1995).
- [3] J. R. Helliwell, and P. M. Rentzepis, Time-Resolved Diffraction (Clarendon Press, New York, 1997)
- [4] H. Ihee, V. A. Lobastov, U. M. Gomez, B. M. Goodson, R. Srinivasan, C. Y. Rua, and A. H. Zewail, *Science* **291**, 458 (2001).
- [5] J. Als-Nielsen, and D. Mc Morrow, Elements of Modern X-Ray Physics (John Wiley & Sons, New York, 2001).
- [6] P. Chen, I. V. Tomov, and P. M. Rentzepis, *J. Chem. Phys.* **104**, 10001 (1996).
- [7] C. W. Siders, A. Cavalleri, K. Sokolowski-Tinten, Ch. Toth, T. Guo, M. Kammler, M. Horn von Hoegen, K. R. Wilson, D. von der Linde, and C. P. J. Barty, *Science* **286**, 1340 (1999).
- [8] Ch. Rose-Petruck, R. Jimenez, T. Guo, A. Cavalleri, C. W. Siders, F. Raksi, J. A. Squier, B. C. Walker, K. R. Wilson, and Ch. P. J. Barty, *Nature* **398**, 310 (1999).
- [9] A. H. Chin, R. W. Schoenlein, T. E. Glover, P. Balling, W. P. Leemans, and C. V. Shank, *Phys. Rev. Lett.* **83**, 336 (1999).
- [10] D. A. Reis, M. F. DeCamp, P. H. Bucksbaum, R. Clarke, E. Dufresne, M. Hertlein, R. Merlin, R. Falcone, H. Kapteyn, M. M. Murnane, J. Larson, Th. Missallia, and J. S. Wark, *Phys. Rev. Lett.* **86**, 3072 (2001).
- [11] A. Rousse, C. Richel, S. Foutmaux, I. Uschmann, S. Sebban, G. Grillon, Ph. Balcou, E. Forster, J.P. Geindre, P. Audebert, J. C. Gauthier, and D. Hulin, *Nature* **410**, 65 (2001).

- [12] Ch. Rischel, A. Rousse, I. Uschmann, P.-A. Albouy, J.-P. Geindre, P. Audebert, J.-Cl. Gauthier, E. Fôrster, J.-L. Martin, and A. Antonetti, *Nature* **390**, 490 (1997).
- [13] S. Techert, F. Schotte, and M. Wulff, *Phys. Rev. Lett.* **86**, 2030 (2001).
- [14] V. Srajer, T. Y. Teng, Th. Ursby, Cl. Pradervand, Zhon Ren, Shin-ichi Adachi, W. Schildkamp, D. Bourgois, M. Wulff, and K. Moffat, *Science* **274**, 172 (1996).
- [15] V. Srajer, Z. Ren, T. Y. Teng, M. Schmidt, T. Ursby, D. Bourgois, C. Pradervand, W. Schildkamp, M. Wulff, and K. Moffat, *Biochemistry* **40**, 13802 (2001).
- [16] B. Perman, V. Srajer, Zhon Ren, T. Y. Teng, Cl. Pradervand, Th. Urby, D. Bourgois, F. Schotte, M. Wulff, R. Kort, K. Hellingwerf, and K. Moffat, *Science* **279**, 1946 (1998).
- [17] Z. Ren, B. Perman, V. Srajer, T. Y. Teng, C. Pradervand, D. Bourgois, F. Schotte, T. Ursby, R. Krot, M. Wulff, and K. Moffat, *Biochemistry* **40**, 13788 (2001).
- [18] R. Neutze, R. Wouts, S. Techert, J. Davidson, M. Koczis, A. Kirrander, F. Schotte, and M. Wulff, *Phys. Rev. Lett.* **87**, 195508 (2001).
- [19] C. P. J. Barty, M. Ben-Nun, Ting Guo, F. Raksi, Ch. Rose-Petruck, J. Squier, K. R. Wilson, V. V. Yakovlev, P. M. Weber, Zhiming Jiang, A. Ikhlef, and J.-Cl. Keiffer, in Ref. 3, p. 44.
- [20] M. Ben-Nun, J. Cao, and K. Wilson, *J. Phys. Chem. A* **101**, 8743 (1997).
- [21] J. Cao, and K. R. Wilson, *J. Phys. Chem.* **102**, 9523 (1998).
- [22] C. H. Chao, S. H. Lin, W. K. Liu, and P. Rentzepis, in Ref. 3, p. 260.
- [23] J. P. Bergsma, M. H. Coladonato, P. M. Edelstein, J. D. Kahn, and K. R. Wilson, *J. Chem. Phys.* **84**, 6151 (1986).
- [24] J. Cao, Ch. J. Bardeen, and K. R. Wilson, *Phys. Rev. Lett.* **80**, 1406 (1998).
- [25] L. D Landau, and E. M. Lifshitz, *Electrodynamics of Continuous Media* (Pergamon Press, London, 1960), p. 398.

- [26] L. Landau, and E. Lifchitz, *Théorie des Champs* (Editions MIR, Moscou 1970), p. 212.
- [27] F. Schotte, S. Techert, P. A. Anfinrud, V. Srajer, K. Moffat, and M. Wulff in *Third Generation Hard X-ray Synchrotron Radiation Sources: Source Properties, Optics, and Experimental Techniques*, D. Mills editor (John Willey & Sons, New York, 2002), chap. 10.
- [28] T. J. Chuang, G. W. Hoffman, and K. B. Eisenthal, *Chem. Phys. Lett.* **25**, 201 (1974).
- [29] D. F. Kelley, N. Alan Abul-Haj, and Du-Jeon Jang, *J. Chem. Phys.* **80**, 4105 (1984).
- [30] A. L. Harris, M. Berg, and C. B. Harris, *J. Chem. Phys.* **84**, 788 (1986).
- [31] A. L. Harris, J. K. Brown, and C. B. Harris, *Ann. Rev. Phys. Chem.* **39**, 341 (1988).
- [32] R. Mulliken, *J. Chem. Phys.* **33**, 288 (1971).
- [33] M. Ferrario, and M. W. Evans, *Chem. Phys.* **72**, 141 (1982).
- [34] G. Ciccotti, and J. P. Ryckaert, *Comput. Phys. Rep.* **4**, 345 (1986).
- [35] D. J. Nesbitt, and J. T. Hynes, *J. Chem. Phys.* **77**, 2130 (1982).
- [36] J. P. Bergsma, M. H. Colodonato, P. M. Edelsten, J. D. Kahn, K. R. Wilson, and D. R. Fredkin, *J. Chem. Phys.* **84**, 6151 (1986).
- [37] F. Mirloup, R. Vuilleumier, and S. Bratos, in preparation.
- [38] S. Tanaka, V. Chernyak, and S. Mukamel, *Phys. Rev. A* **63**, 063405 (2001).
- [39] I. V. Tomov, D. A. Oulianov, P. Chen, and P. M. Rentzepis, *J. Phys. Chem. B* **103**, 7081 (1999).

List of Figures

- 1 The liquid sample, contained in a cubic box Σ , is divided into a large number of small cubic cells Σ' . Their dimension L is large as compared with the length l which is probed, but small as compared with the wave length λ of the incident radiation. The system contained in Σ is then dynamically equivalent to an ensemble of sub-systems contained in different cells Σ' 29
- 2 Electronic energy surfaces of I_2 . Only four of ten electronic states correlating with the ground electronic state X of I_2 are illustrated. R_X indicates the inter-atomic separation of two iodine atoms in the state X of I_2 , $R_{A/A'}$ indicates that distance in the states A,A', whereas R_0 gives the length of the extended hot molecule I_2^* 30
- 3 Recombinaison processes of iodine in molecular solvents. The process α leads to non-geminate recombinaison and the processes β and γ to geminate recombinaison. 31
- 4 Comparison between molecular dynamics and model calculations. The system under consideration is a mixture I_2/CH_2Cl_2 ; its molecular dynamics are governed by an empirical potential. Full curves represent results of the model (see text) and dotted curves those of Molecular Dynamics simulations. Diffraction signals $S(\mathbf{q}, t)/P$ in Figs. 4.a,b correspond to time delays equal to 1 ps and 25 ps respectively. In order to facilitate the comparison, only the process γ was considered. 32
- 5 Time-resolved diffraction patterns $\Delta S(\mathbf{q}, \tau)/P$ of the mixture I_2/CH_2Cl_2 . Figs. 5.a,b,c correspond to three different values of the scattering vector \mathbf{q} . These patterns vary appreciably when going from one value of \mathbf{q} to another, and the signal may even change its sign. In Fig. 5.c, the solid line represents the theoretical result of the present study, while the points with error bars correspond to the experimental result of Neutze et al.¹⁸ 33

- 6 Wave-vector-resolved diffraction patterns $\Delta S(\mathbf{q}, \tau)/P$ of the mixture $\text{I}_2/\text{CH}_2\text{Cl}_2$. Figs. 6.a,b,c correspond to three different time delays τ . Only the hole contributes to the signal of Fig. 6.a; the hole and molecules populating the states A/A' of I_2 contribute to the signal of Fig. 6.b, whereas the hole, the states A/A' of I_2 and the extended molecule I_2^* contribute to the signal of Fig. 6.c. In Fig. 6.b, the smooth solid line represents the theoretical result of the present study, while the broken line corresponds to the experimental result of Neutze et al.¹⁸ 34
- 7 Wave-vector-resolved diffraction pattern $\Delta S(\mathbf{q}, \tau)/P$ of the mixture I_2/CCl_4 , calculated for three time delays equal to 0, 100 and 500 ps. Fig. 7.a represents $\Delta S(\mathbf{q}, \tau)_{inst}$ and thus neglects the effect of X-ray pulse duration; and Fig. 6.b includes this effect. Real time motions of iodine atoms manifest themselves by shifting positive and negative peaks of the diffraction patterns to higher \mathbf{q} values. 35

Figure 1: S. Bratos et al., Time-Resolved X-Ray Diffraction ...

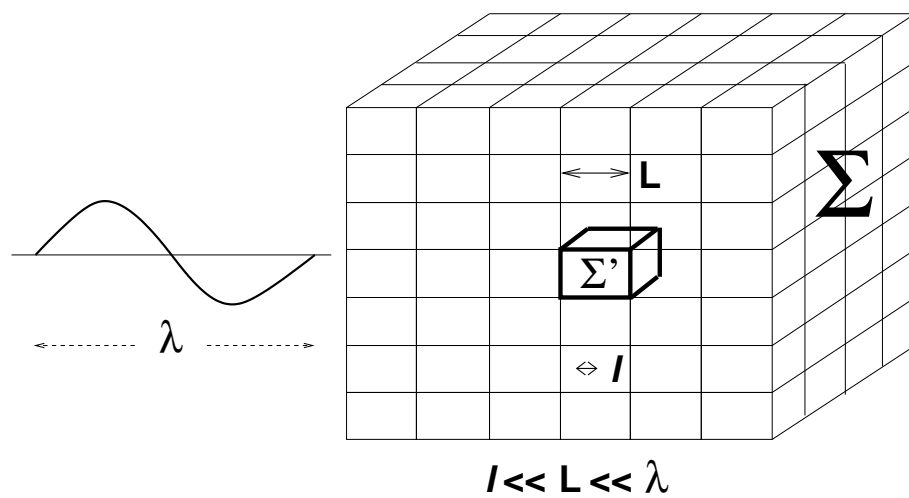


Figure 2: S. Bratos et al., Time-Resolved X-Ray Diffraction ...

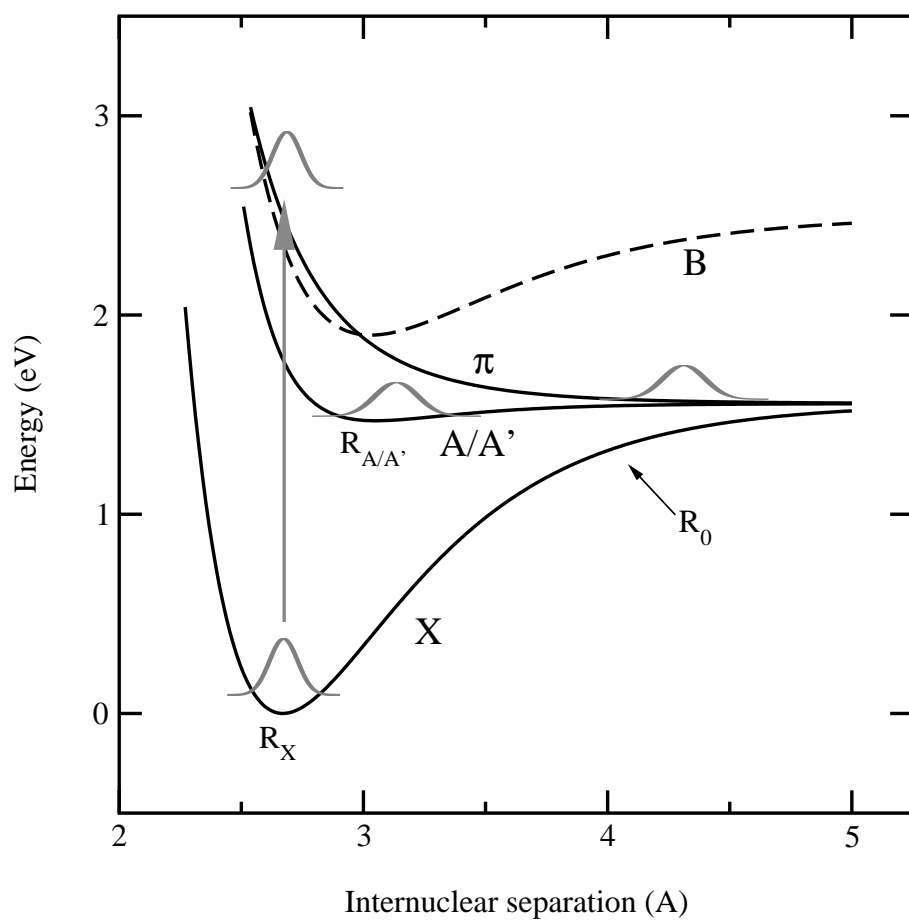


Figure 3: S. Bratos et al., Time-Resolved X-Ray Diffraction ...

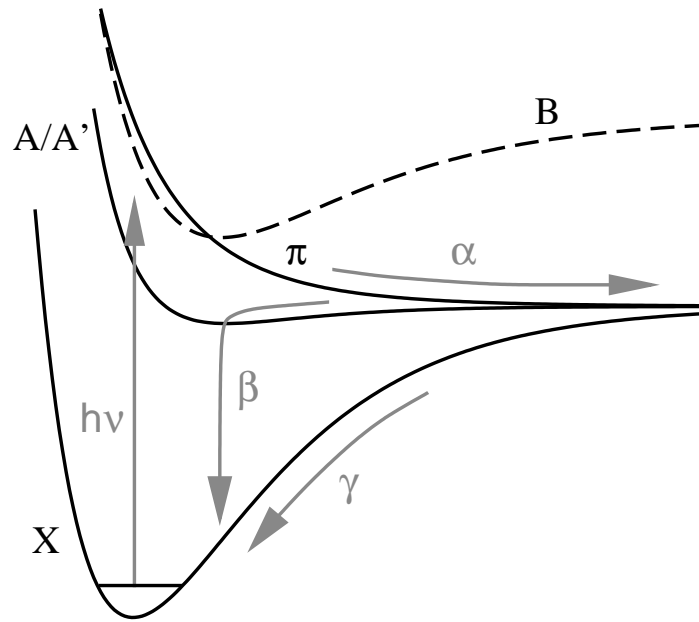


Figure 4: S. Bratos et al., Time-Resolved X-Ray Diffraction ...

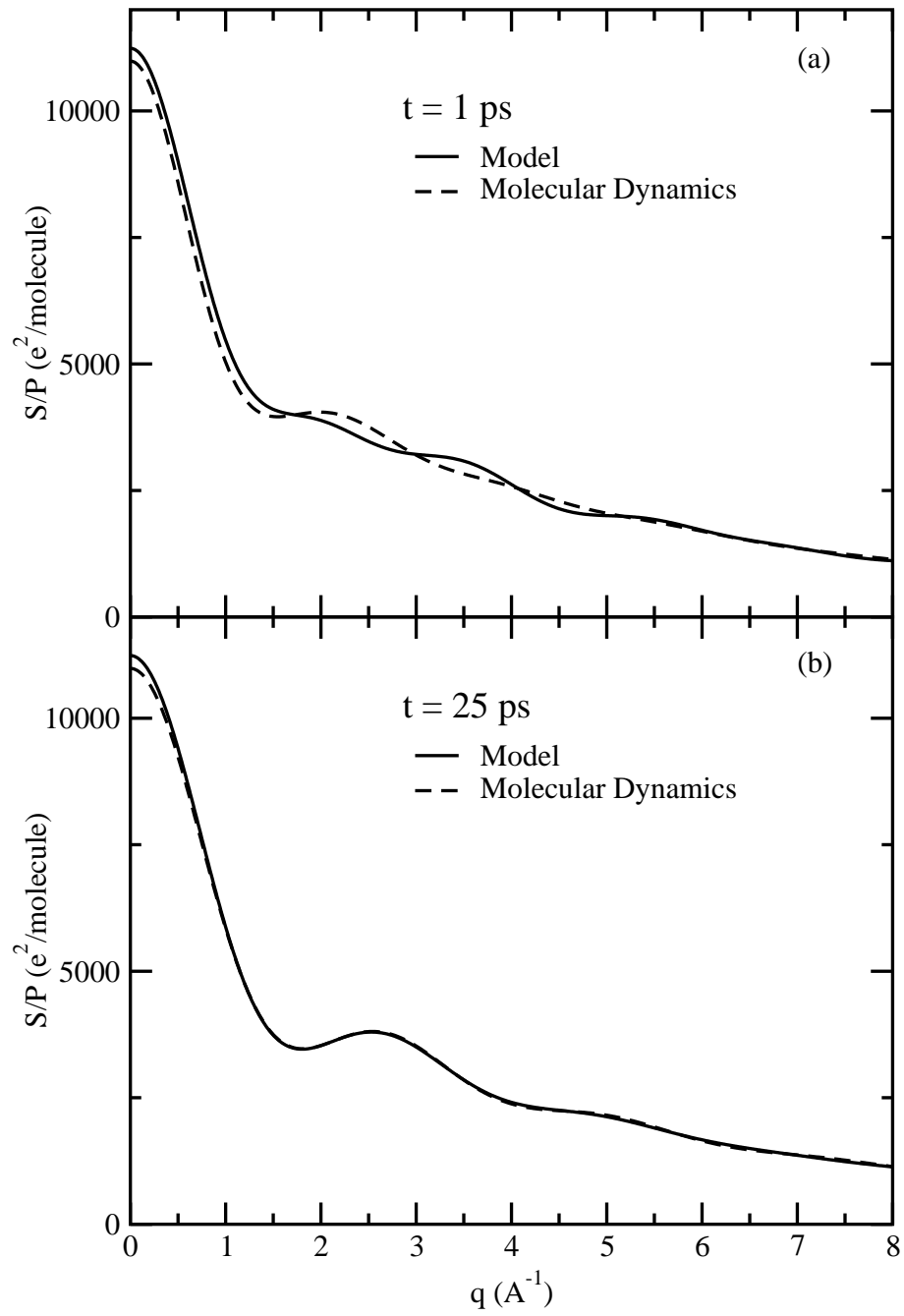


Figure 5: S. Bratos et al., Time-Resolved X-Ray Diffraction ...

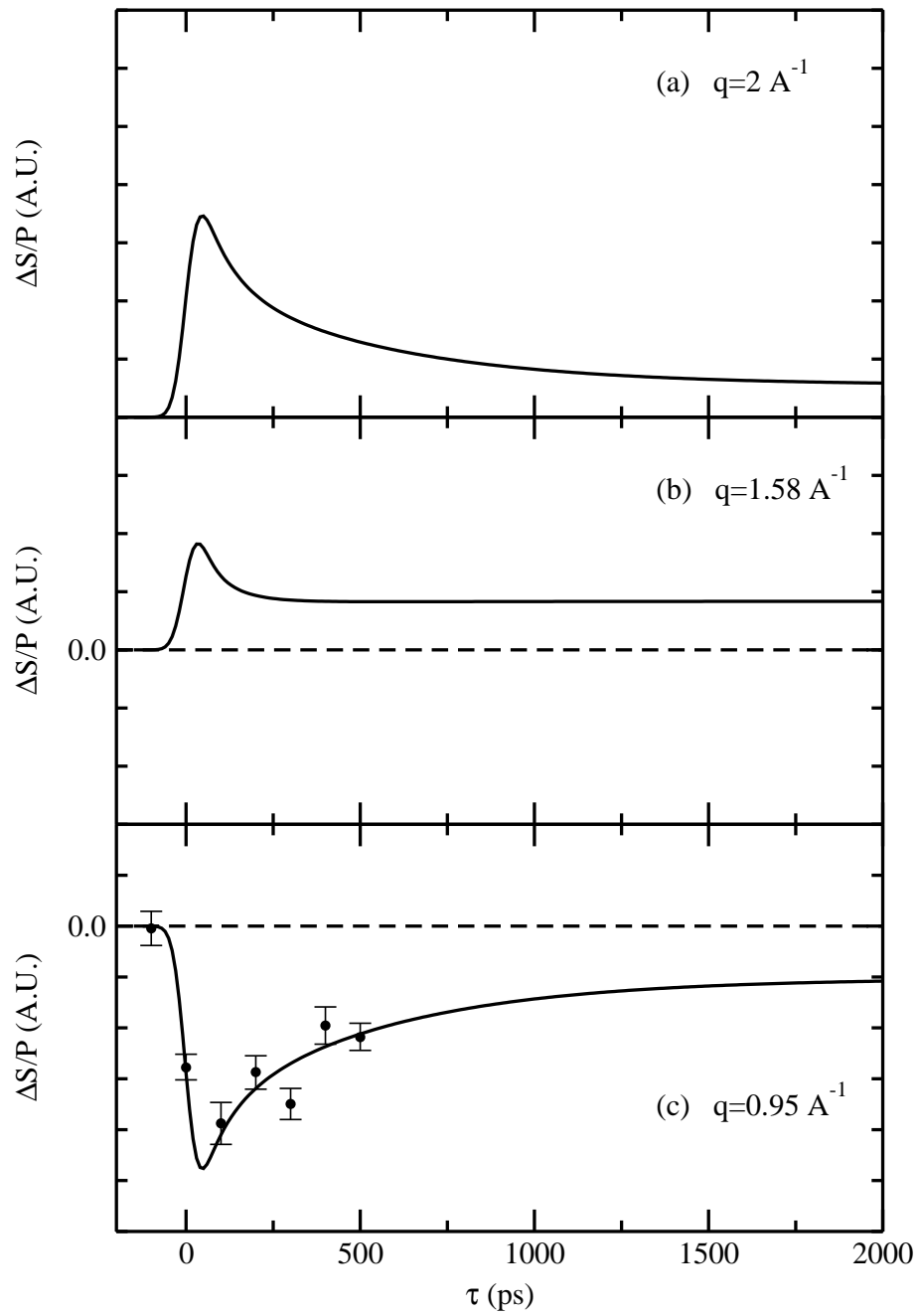


Figure 6: S. Bratos et al., Time-Resolved X-Ray Diffraction ...

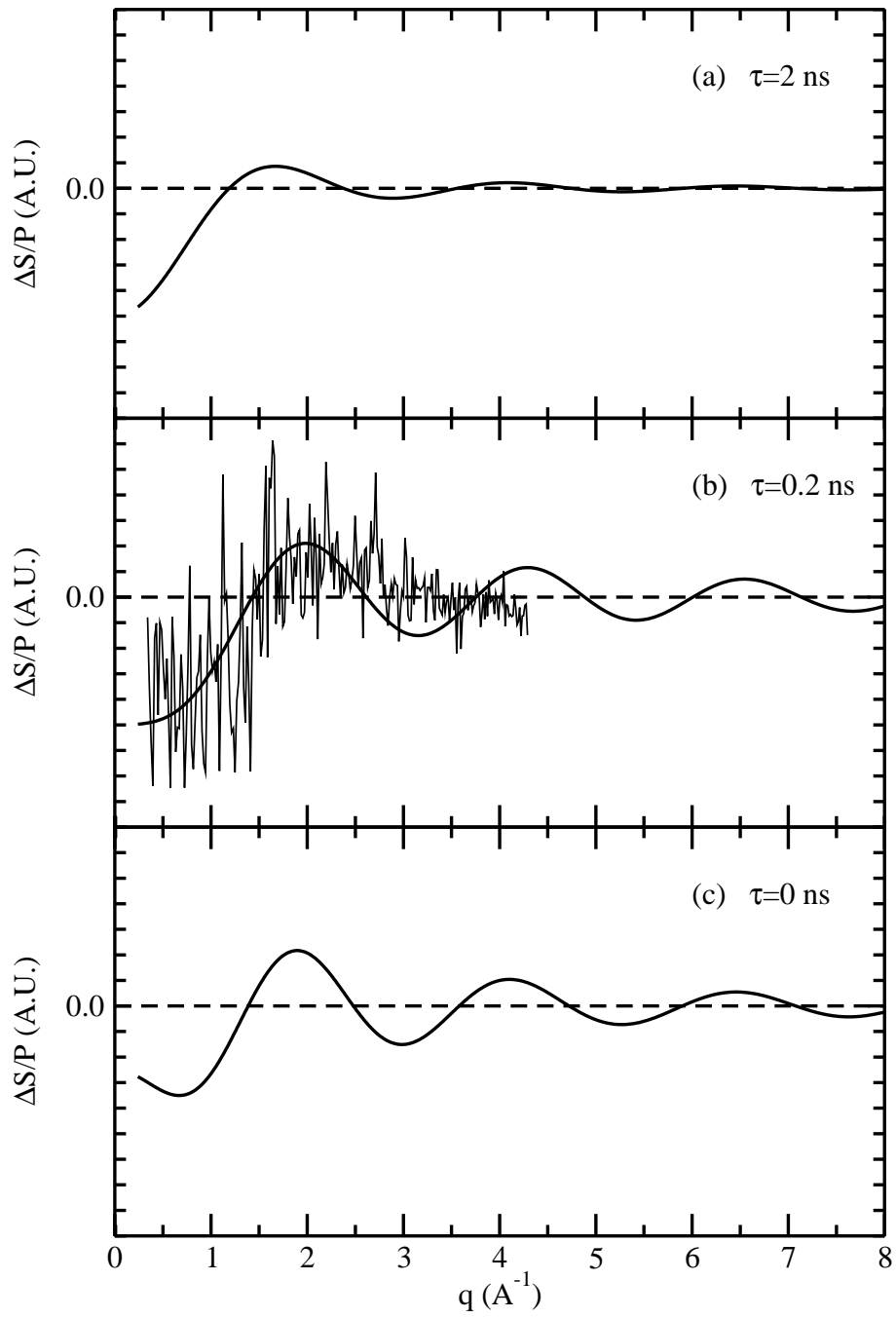


Figure 7: S. Bratos et al., Time-Resolved X-Ray Diffraction ...

